Femtosecond interferometric autocorrelations in the presence of pulse front distortions

F. Grasbon[1], A. Dreischuh [1,2], G.G. Paulus [1], F. Zacher [1], and H. Walther [1,3]

[1]MPI für Quantenoptik, Hans-Kopfermann-Str. 1, 85748 Garching, Germany

[2]Sofia University, Dept. of Quantum Electronics, 5, J. Bourchier Blvd, 1164 Sofia, Bulgaria

[3]Sektion Physik der Universität München, Am Coulombwall 1, 85747 Garching, Germany

ABSTRACT

The tilt of the pulse front caused by misalignment in stretcher-compressor devices which are used in chirped pulse amplification should be carefully considered in the design of femtosecond laser systems. We present a convenient procedure for online measurement and minimization of the tilt in a grating stretcher/compressor setup. In addition, we present a theoretical model for the autocorrelation signal in the presence of pulse front distortion. The influence of the pulse front tilt to the autocorrelation function is numerically simulated and compared with the case for pulses with fourth order chirp.

Keywords: femtosecond pulse, interferometric autocorrelation, pulse front distortion, chirp

1. INTRODUCTION

The tilt of the pulse front is one of the major issues in chirped pulse amplification (CPA) systems.[1-3] Pulse front distortion can also occur when femtosecond pulses are focused[4,5] or passed through birefringent crystals.[6] It leads to an undesired increase of the effective pulse duration and is accompanied by spatial chirp. Further, it can substantially reduce the accuracy of interferometrically measured optical nonlinearities.[7] Even the overlap of femtosecond pulses over their intensity profile in space is not a trivial problem anymore.[8]

2. AUTOCORRELATION AND PULSE FRONT DISTORTION

An exact measurement of the pulse in time and space is required for applications using high-power short pulse laser systems.

2.1. Physical situation

The conventional Michelson interferometer (Fig. 1a) is not sensitive to a distortion of the pulse front. Since the two pulses are tilted parallelly,, their overlap in the nonlinear crystal for second harmonic (SH) generation depends only on the time delay τ_d. The modification of the correlator by flipping one of the beams (as in the Mach-Zehnder scheme, Fig. 1b) results in a space time coupling. Fig. 2 shows this situation. It is easily seen that the effective pulse length will be longer than τ_0; therefor a change in the autocorrelation signal will appear. The influence of the tilted pulse front to the interference of two pulses is shown in Fig. 3. Depending on the pulse overlap (Fig. 3, top), interference lines are obtained on one side first, then mainly at the center of the beam cross-section, and finally on

Figure 1. Conventional Michelson (a) and Mach-Zehnder autocorrelator with flipping one beam horizontally (b). Dotted lines: tilted pulses (parallel (a) and antiparallel (b) pulse front orientation at the entrance of the SHG crystal).

SPIE Vol. 3571 • 0277-786X/99/$10.00

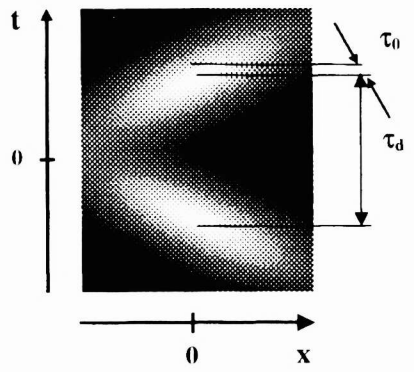

Figure 2. Space time coupling: relative position of two pulses with pulse length τ_0 and time delay τ_d.

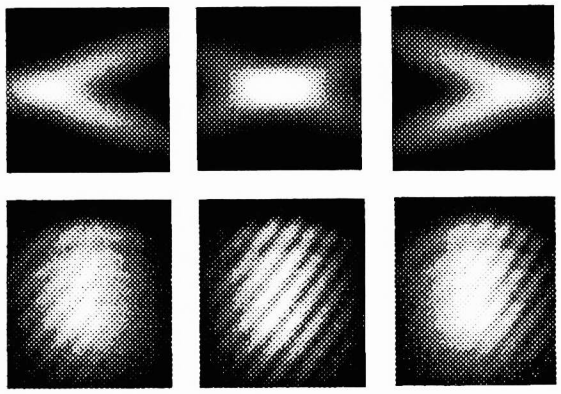

Figure 3. Top: space time dependent delay $\tau_d = -\tau$ (left), 0(center), and τ (right) between pulses with tilted fronts. Bottom: the corresponding interference pattern (experimental data).

the other side of the beam (Fig. 3, bottom). The experimental interference pictures presented in Fig. 3 (bottom) are obtained by a Ti:Sapphire CPA laser system and a modified Mach-Zehnder interferometric autocorrelator (Fig. 1b). The interpretation of the corresponding second order autocorrelation trace is strongly handicapped by the tilt (section 2.3), in particular in combination with higher order chirps (section 4). However, the interference pattern makes it much easier to estimate the magnitude of the tilt and provides a convenient procedure for the tilt correction (section 3.1).

2.2. Theoretical model

Let us consider the interferometric autocorrelation between ultrashort pulses of equal durations $\tau_{0,\mathcal{E}}$ and symmetrical, but opposite pulse front tilts α, as in the situation at the modified autocorrelator (Fig. 1b). Starting with the optical field amplitudes $\mathcal{E}_1$ and $\mathcal{E}_2$ for the two pulses in the form

$$\mathcal{E}_1 = A_t(t - \tau_d - \alpha x)A_r(x)\exp\{i\omega(t - \tau_d)\} \qquad \mathcal{E}_2 = A_t(t - \tau_d - \alpha x)A_r(x)\exp\{i\omega t\} \tag{1}$$

the calculated intensity $I_{2\omega}(t, \tau_d, \alpha x) = |(\mathcal{E}_1 + \mathcal{E}_2)^2|^2$ of the second harmonic that is generated during the autocorrelation is

$$\begin{aligned} I_{2\omega}(t, \tau_d, \alpha x) \;=\; & A_r^4(x)\Big\{A_t^4(t + \alpha x) + A_t^4(t - \tau_d - \alpha x) + 4A_t^2(t + \alpha x)A_t^2(t - \tau_d - \alpha x) + \\ & 4\left[A_t^3(t + \alpha x)A_t(t - \tau_d - \alpha x) + A_t(t + \alpha x)A_t^3(t - \tau_d - \alpha x)\right]\cos(\omega_0\tau_d) + \\ & 2A_t^2(t + \alpha x)A_t^2(t - \tau_d - \alpha x)\cos(2\omega_0\tau_d)\Big\}. \end{aligned} \tag{2}$$

With a wide aperture photodetector and a detector signal rise time much longer than the typical pulse length, the normalized correlation signal is of the form

$$P_{2\omega}^{\mathrm{AK}}(\tau_d, \alpha) = \frac{\int_{-\infty}^{\infty}\int_{-\infty}^{\infty} I_{2\omega}(t, \tau_d, \alpha x)\,dtdx}{\int_{-\infty}^{\infty}\int_{-\infty}^{\infty} |\mathcal{E}_i^2|^2\,dtdx}, \tag{3}$$

where $i = 1$ or 2. The natural normalization to the energy of the SH signal generated from each pulse separately yields a correlation peak-to-background ratio of 8:1 at zero tilt of the pulse front.

The exact solution of equation 3 for a Gaussian beam/pulse allows some insight to the the influence of the pulse front distortion α on the effective pulse duration τ_{eff}. For this case equation 3 becomes

$$\begin{aligned} P_{2\omega}^{\mathrm{AK}}(\tau_d, \alpha) \;=\; & 1 + \frac{\tau_{0,\mathcal{E}}}{\sqrt{\tau_{0,\mathcal{E}}^2 + \alpha^2 x_{0,\mathcal{E}}^2}}\exp\left\{-\frac{\tau_d^2}{\tau_{0,\mathcal{E}}^2 + \alpha^2 x_{0,\mathcal{E}}^2}\right\}\left[2 + \cos(2\omega_0\tau_d)\right] + \\ & \frac{8\tau_{0,\mathcal{E}}}{\sqrt{4\tau_{0,\mathcal{E}}^2 + 3\alpha^2 x_{0,\mathcal{E}}^2}}\exp\left\{-\frac{3\tau_d^2}{4\tau_{0,\mathcal{E}}^2 + 3\alpha^2 x_{0,\mathcal{E}}^2}\right\}\cos(2\omega_0\tau_d) \end{aligned} \tag{4}$$

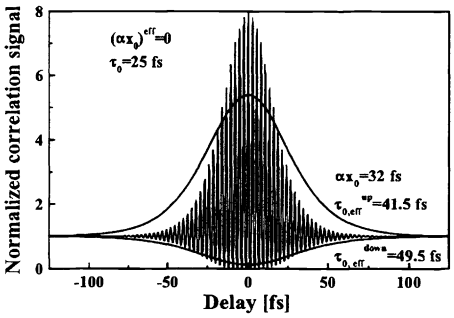

Figure 4. Comparison of the interferometric autocorrelation traces for Michelson and modified Mach-Zehnder (envelope) autocorrelator.

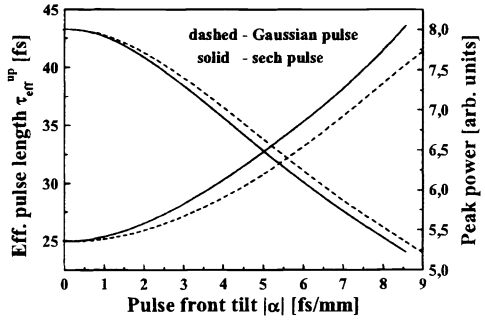

Figure 5. Increase of the effective pulse length and decrease of the peak interferometric autocorrelation signal vs. pulse front tilt.

where $\tau_{0,\mathcal{E}}$ and $x_{0,\mathcal{E}}$ are the half width of the field of the pulse in time and space. The autocorrelation function $P_{2\omega}^{AK}(\tau_d, \alpha)$ and therefor the effective pulse duration τ_{eff} are now functions of $\tau_{0,\mathcal{E}}$ and $\alpha x_{0,\mathcal{E}}$: $\tau_{\text{eff}} = \tau_{\text{eff}}(\tau_{0,\mathcal{E}}, \alpha x_{0,\mathcal{E}})$.

2.3. Numerical results

The Michelson and the modified Mach-Zehnder autocorrelators give quite different interferometric autocorrelation signals for the same pulse front angular tilt. Obviously, the presence of a tilt in the pulse front affects the autocorrelation peak-to-background ratio and the effective pulse duration. The peak-to-background ratio is longer than 8:1, while the background keeps its strength and can be used for calibration (Fig. 4). The effective pulse duration $\tau_{\text{eff}}^{\text{up}}$ is determined from the autocorrelation pulse width measured at half of the peak-to-background difference. However, the envelope for destructive interference of the autocorrelation trace does not contain information that is easy to interpret because of the rather poor signal to noise ratio. Note that x_0 and τ_0 (Fig. 4) are the full width of the intensity distribution in space and time, in contrast to $\tau_{0,\mathcal{E}}$ and $x_{0,\mathcal{E}}$.

The monotone increasing function plotted in Fig. 5 presents the dependence of the effective pulse duration $\tau_{\text{eff}}^{\text{up}}$ on the pulse front tilt α. The increase in the effective pulse length is accompanied by a decrease of the SH peak power. In general, the autocorrelation of a Gaussian pulse is less affected by a pulse front distortion than that of a sech pulse with the same length τ_0. Despite that pulses from mode locked lasers are assumed to be sech shaped ,the previous result is important since higher order dispersion is able to reshape these pulses towards Gaussian pulses.

3. TILT ANGLE MEASUREMENT AND ALIGNMENT

The interference picture of the modified Mach-Zehnder interferometer allows a quick measurement of the tilt angle in one axis. Furthermore, it can be used for the alignment of the laser system to minimize the tilt of the pulse front. A horizontal misalignment of mirror M2 in the interferometer by some angle introduces an additional relative tilt of the two pulse fronts in the two arms of the interferometer. The interference pattern appears for pulses (regardless of any intrinsic tilt) on one side and develops over the beam cross section to the other side when the relative time delay τ_d is changed. This tilt can be controlled by mirror M2 and is used for the tilt measurement.

3.1. Procedure for tilt angle measurement

At first the Mach-Zehnder interferometer is aligned to see the central part of the interference pattern. Then the two beams are aligned parallelly. In the case of an intrinsic tilt of the pulse front by α, this intrinsic tilt can compensate the tilt introduced by the misalignment of mirror M2 by an angle of 2β if $\alpha = -\beta$. If this condition is fulfilled, the interference lines appear and disappear simultaneously over the beam cross section when the relative time delay τ_d is changed. The number of interference lines per unit length (1/D) gives the angle α of the intrinsic pulse front tilt (e.g. in fs/mm)

$$\alpha = \arcsin(\frac{\lambda}{2D}), \tag{5}$$

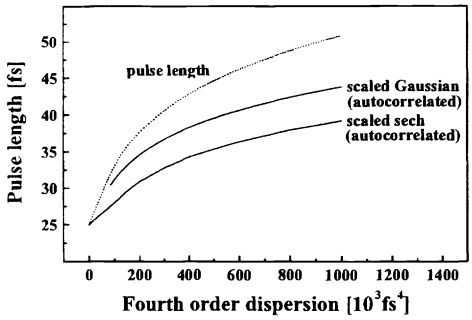

Figure 6. True pulse length and autocorrelation length scaled for sech and Gaussian pulses.

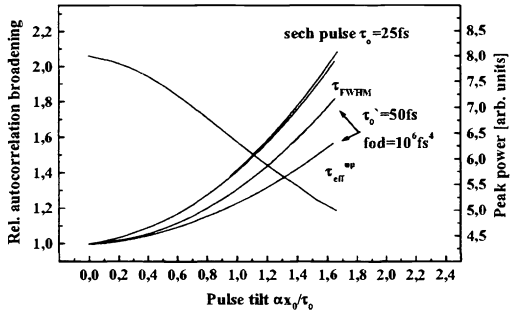

Figure 7. Relative autocorrelation broadening (FWHM τ_{FWHM} and above background envelope FWHM $\tau_{\text{eff}}^{\text{up}}$) and peak power vs. relative pulse front tilt for a 25fs sech pulse and the same pulse stretched to 50fs by FOD.

where D is the distance between two interference maxima. The accuracy of the measurement is given by the resolution of the fringes (in the order of 1fs/mm).

3.2. Compressor alignment

The geometry of our commercial compressor is vertically asymmetric for the two passes by construction and results in a vertical pulse front tilt. An additional horizontal tilt is mainly due to the accuracy of a retroreflector. The horizontal tilt was varied from 0fs up to about 50fs over the beam diameter x_0. By looking at the change of the interference picture, the pulse front distortion induced by the compressor can be minimized in each axis. Our compressor compensates for the second and third order dispersion of the stretcher and regenerative amplifier, but it leaves a non negligible fourth order dispersion (FOD). In the next section this chirp is included to the numerical autocorrelation including pulse front tilt.

4. FOD-CHIRP AND PULSE FRONT TILT

The ratio of the autocorrelation length to the pulse length depends on the chirp. This is shown in Fig. 6 for a 25fs sech shaped pulse. The scaled autocorrelation pulse length assuming a Gaussian and a sech pulse form underestimates the true pulse length. The deviation exceeds soon 10 percent. The pulse envelope in time changes with increasing FOD chirp towards a Gaussian shape, so that the Gaussian scaling factor is more appropriate for a small FOD chirp. In Fig. 7, a pulse front tilt is included for a 25fs pulse and a FOD chirped pulse (pulse duration 50fs). The influence of the pulse front tilt on the autocorrelation of the chirped pulse is smaller than for an unchirped pulse. This is due to the weaker interference in the wings due to the frequency chirp. Furthermore, the broadening of the autocorrelation depends on the level where the autocorrelation length is taken. Since the peak-to-background ratio of 8:1 is not given anymore, the experimental measurement of the autocorrelation length should be taken at the half maximum above background. The resulting pulse length is called $\tau_{\text{eff}}^{\text{up}}$. This value is compared to the FWHM of the autocorrelation trace and shows to be less influenced by the tilt for the FOD chirped pulse. Additionally, the decrease of the peak power is indicated in Fig. 7.

5. CONCLUSIONS

In the interferometric autocorrelation curves obtained by the conventional Michelson and Mach-Zehnder interferometers, the tilt of the pulse front remains obscured. The effective pulse duration can be substantially larger. An accurate approach should involve an interferometric autocorrelator where the beam is flipped successively in both axes. The tilt of the pulse front is accompanied by a spatial chirp. The higher order dispersion leads to an undesired reshaping of the pulse and the autocorrelation signal. The broadening of the autocorrelation signal due to the pulse front tilt is not as effective.

ACKNOWLEDGMENTS

A.D. is grateful to the Alexander von Humboldt-Foundation (Germany) for the award of a fellowship and for the opportunity to work in the stimulating atmosphere of the Max-Planck-Institut für Quantenoptik (Garching, Germany).

REFERENCES

1. O. Martinez, "Pulse distortions in tilted pulse schemes for ultrashort pulses," *Opt. Commun.* **59**, pp. 229–232, 1986.
2. C. Fiorini, C. Sauteret, C. Rouyer, N. Blanchot, S. Seznec, and A. Migus, "Temporal aberrations due to misalignments of a stretcher-compressor system and compensation," *IEEE J.Quant.Electron.* **QE-30**, pp. 1662–1670, 1994.
3. A. Kasper, G. Pretzler, and K. Witte, "100 or 300fs? Unnoticed pulse lengthening in the focus resulting from a tilted pulse front at the exit of a cpa-laser system," *Verhandlungen der DPG* **(VI) 33**, p. 223, 1998.
4. C. Radzewicz, M. la Grone, and J. Krasinski, "Interferometric measurement of femtosecond pulse distortion by lenses," *Optics Communications* **126**, pp. 185–190, 1996.
5. S. Ameer-Beg, A. Langley, I. Ross, W. Shaikh, and P. Taday, "An achromatic lens for focusing femtosecond pulses: direct measurement of femtosecond pulse front distortion using a second-order autocorrelation technique," *Optics Communications* **122**, pp. 99–104, 1996.
6. C. Radzewicz, J. Krasinski, M. la Grone, M. Trippenbach, and Y. Band, "Interferometric measurement of femtosecond wave-packet tilting in rutile crystal," *J.Opt.Soc.Am.* **B14**, pp. 420–424, 1997.
7. G. Shukan, R. G. Ispasoiu, A. M. Fox, and J. F. Ryan., "Ultrafast two-photon nonlinearities in CdSe near 1.5 μm studied by interferometric autocorrelation," *IEEE J.Quant.Electron.* **QE-34**, pp. 1374–1379, 1998.
8. A. Maznev, T. Criminus, and K. Nelson, "How to make femtosecond pulses overlap," *Opt. Lett.* **23**, pp. 1376–1378, 1998.